O. KRYSHTAL*#, A. KRUK*, F. MAO**, M. TAHER**,***, U. JANSSON**,
A. CZYRSKA-FILEMONOWICZ*

MICROSTRUCTURE AND PHASE COMPOSITION OF THE Ag–Al FILM WEAR TRACK: THROUGH-THICKNESS CHARACTERIZATION BY ADVANCED ELECTRON MICROSCOPY

Analytical transmission electron microscopy has been applied to characterize the microstructure, phase and chemical composition of the Ag–Al wear track throughout its thickness down to the atomic level. Microscopy findings have been correlated with Ag–Al film tribological properties to understand the effect of the hexagonal solid solution phase on the tribological properties of this film. Ag–25Al (at.%) films have been produced by simultaneous magnetron sputtering of components in Ar atmosphere under 1 mTorr pressure and subjected to pin-on-disc tribological tests. It has been shown that hcp phase with (001) planes aligned parallel to the film surface dominates both in as-deposited and in tribofilm areas of the Ag–Al alloy film. Possible mechanisms of reduced friction in easily oxidized Ag–Al system are discussed and the mechanism based on readily shearing basal planes of the hcp phase is considered as the most probable one.

Keywords: Ag–Al alloy; TEM; EDX; hexagonal phase; electrical contact

1. Introduction

Ag is widely used in electrical contacts due to its excellent electrical properties. However, Ag in pure form has drawbacks since it is too soft and exhibits a high mechanical wear rate, leading to a limited lifetime of the contact pads. This also adds cost to the product since the price of Ag is high. Another disadvantage of Ag to be used in sliding electrical contact applications is that it is prone to material transfer and to cladding a counter surface during sliding, then creating an Ag−Ag contact. The friction coefficient of such a contact in a dry sliding system is high (>1) [1]. The Ag cladding and the resulting high friction can cause unstable performance of a device, or even its failure due to an electrical short-circuit between adjacent current paths. Consequently, there is a need for new sliding electrical contact materials that combine good electrical properties, such as low electrical resistivity and low electrical contact resistance, with good tribological properties such as low friction coefficient and low wear rate.

In our previous works, on the development of new electrical contact materials with improved tribological properties, we have investigated the correlations between phase structure and the tribological properties of Ag-based alloys both in thin film and in bulk forms [2-4]. It has been found that the presence of the hcp phase in Ag−X (X = Al, In or Sn) alloys could significantly reduce the friction coefficient and wear rate of Ag. This effect has also been previously reported in some hcp-metals (La, Re, Co, etc.) [5, 6]. The detailed mechanism behind this needs more investigation; however, two major hypotheses can be envisioned: (i) easy-shearing planes parallel to the sliding direction; (ii) formation of oxide tribofilm during sliding conducive to low friction. A sliding-induced alignment of easy-shearing planes parallel to the sliding direction had been previously observed in a low-friction Ag−In bulk alloy with the presence of hcp phase [3]. Since Ag−Al alloy is more sensitive to oxidation than the Ag−In alloy [3], it will be interesting to see if the alignment of easy-shearing planes can also be observed in the easy-oxidation Ag−Al alloy or if oxide formation is responsible for the reduced friction.

Therefore, in this work, we have focused on characterization of the Ag−Al alloy film wear track by means of advanced electron microscopy and spectroscopy techniques with the intention to gain further insight into a mechanism of low friction of the Ag−Al hexagonal solid solution phase.

* AGH UNIVERSITY OF SCIENCE AND TECHNOLOGY (AGH-UST), INTERNATIONAL CENTRE OF ELECTRON MICROSCOPY FOR MATERIAL SCIENCE AND FACULTY OF METALS ENGINEER-
ING AND INDUSTRIAL COMPUTER SCIENCE, AL. MICKIEWICZA 30, 30-059 KRAKÓW, POLAND
** UPPSALA UNIVERSITY, DEPARTMENT OF CHEMISTRY-ÅNGSTRÖM LABORATORY, UPPSALA, SWEDEN
*** INSULATION AND MATERIALS TECHNOLOGY, ABB AB, CORPORATE RESEARCH, VÄSTERÅS, SWEDEN

Corresponding author: kryshtal@agh.edu.pl

2. Experimental procedure

2.1. Sample deposition

Ag−Al films with Al content ca 25 at.% have been formed by simultaneous deposition of components in a custom-built magnetron sputtering system with a base pressure below 9×10^{-9} Torr (details are available elsewhere [2]). The alloy film deposition has been carried out at a rate of ≈0.2 nm/s on a steel plate with a predeposited thin Ti layer. The Ar pressure during deposition was 1 mTorr and the Ar flow was equal to 5 sccm. The substrate has been kept at room temperature and at a floating potential during the deposition process.

2.2. Friction test

The friction coefficients of the Ag−Al film deposited on steel with 25 at.% Al have been measured by pin-on-disc tests using reciprocating movements, by pressing the upper stationary copper pin (Ø =10 mm made of Cu) plated with ca. 20 μm Ag coating towards the specimen. The tribological tests have been performed under dry condition without any lubricant in ambient atmosphere at room temperature, under 2 N load with sliding speed of 3 cm/s. Friction tests are described in detail in Refs [2,3].

The typical friction coefficient was around 0.2, while the pure Ag films typically exhibit high value >1 [2,3].

2.3. Electron microscopy techniques

Microstructure characterization of the Ag–Al film track has been performed with the use of scanning- and (scanning) transmission electron microscopy (SEM, (S)TEM, respectively). High resolution SEM (Merlin Gemini II of ZEISS) has been used to investigate the surface morphology of the film outside and inside the wear track. SEM imaging has been performed with the use of secondary electrons (SE) under a probe current of 1 nA. Cross-section lamella for TEM investigation has been cut from the middle of the wear track using focused ion beam (FIB) NEON CrossBeam 40EsB SEM from ZEISS. Electron-beam induced Pt film (e-Pt) followed by ion-beam induced Pt (i-Pt) layer have been deposited on the Ag−Al film just before cutting the lamellae in order to prevent damage of the film surface with FIB. Images with high angle annular dark field detector (HAADF) in STEM, Energy Dispersive X-Ray Spectroscopy (EDX) chemical element maps and selected area diffraction patterns (SAED) have been acquired using a probe Cs-corrected FEI Titan[3] G2 60-300 transmission electron microscope equipped with ChemiSTEM technology (FEI) at 300kV. Probe currents of 80 pA and 500 pA with a beam convergence angle of 20 mrad have been used for imaging and EDX mapping correspondingly in most of the experiments. A Cliff-Lorimer standardless method has been used for quantification of EDX spectra.

Identification of phases has been performed by electron diffraction and fast Fourier transform (FFT) patterns of high-resolution STEM (HRSTEM) images with the help of the JEMS software package [7].

3. Results and discussion

Figure 1 shows SEM image of as-deposited Ag−Al alloy film and the wear track at different magnifications. Grains with the size of a few tens of nanometers are clearly identified in the as-deposited film, while the wear track is characterized by a rather smooth surface. Figure 2 presents a low-magnification HAADF-STEM image of the FIB lamella cut from the Ag−Al wear track. Ti support layer, as-deposited film and tribofilm area as well as corresponding interfaces are clearly distinguished. The characteristic features of the film microstructure are columnar grains, round nanoparticles and pores. The columnar structure is a typical zone 1-like microstructure [8] obtained due to low deposition temperature (to be discussed later). EDX maps of chemical elements are presented in Fig. 3. One can see that Ag and Al are uniformly distributed throughout the film thickness giving the average composition of the film (both a matrix and small precipitates) of 24 at.% Al. There is no difference in chemical composition between as-deposited and tribofilm areas. A pore area located in the middle of the map is enriched with aluminum and oxygen. An increased content of Al is also observed along the columns of the grain boundaries of the as-deposited film. However, no change in oxygen content has been detected in this region, as follows from the line composition profile shown in Fig. 3e.

Electron diffraction studies showed that as-deposited film has highly textured polycrystalline AgAl hcp phase. Fig. 4a presents a typical diffraction pattern (SAED) from the as-deposited region of the Ag–Al lamellae cut out of the deposited film. HRSTEM images of fiber-like grains reveal the atomic layers with the interplanar spacing of 0.24 nm that corresponds to (002) planes of Ag−Al hcp lattice (representative image is shown in
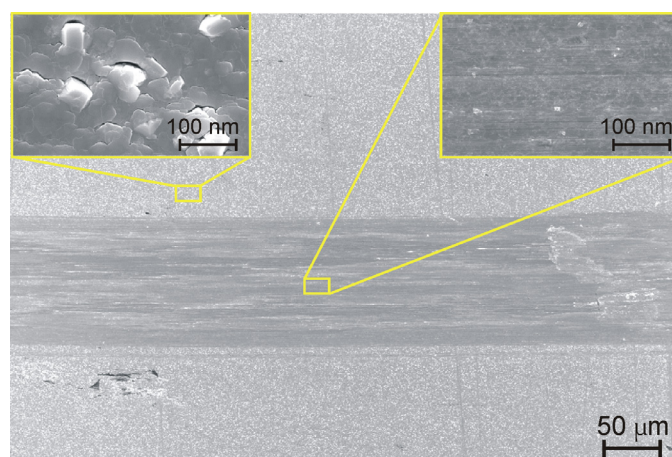

Fig. 1. SEM image of the Ag–Al alloy film with a wear track. Insets show the surface morphology inside and outside of the wear track
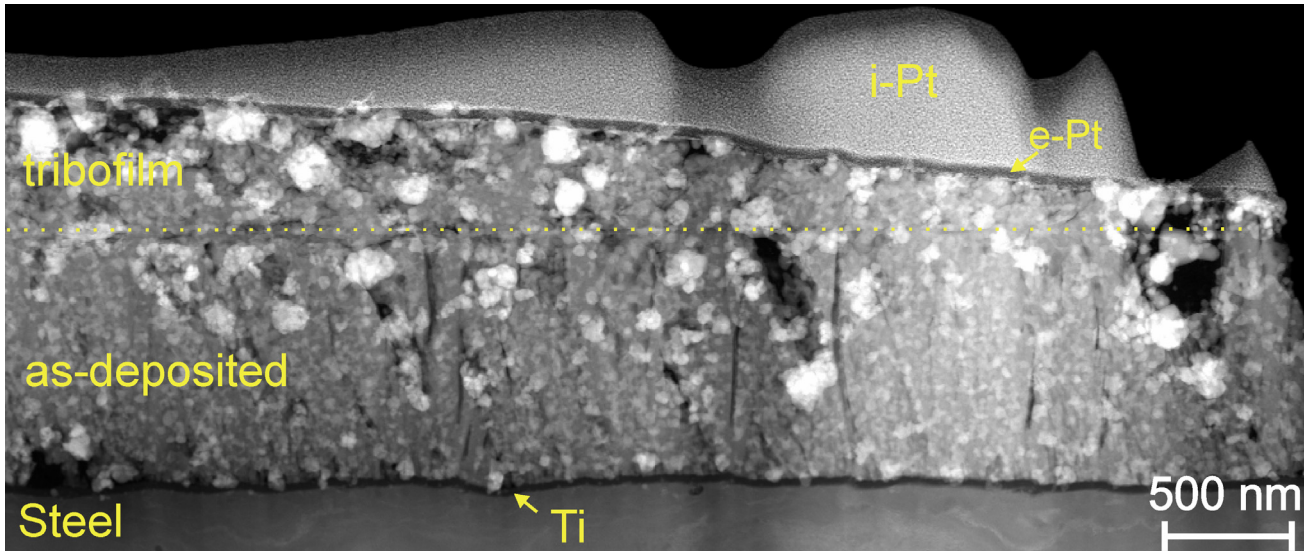
Fig. 2. HAADF-STEM image of the cross-section of the Ag–Al wear track. Interface between tribofilm and as-deposited layer is highlighted with dot line. Sliding direction is normal to the image plane
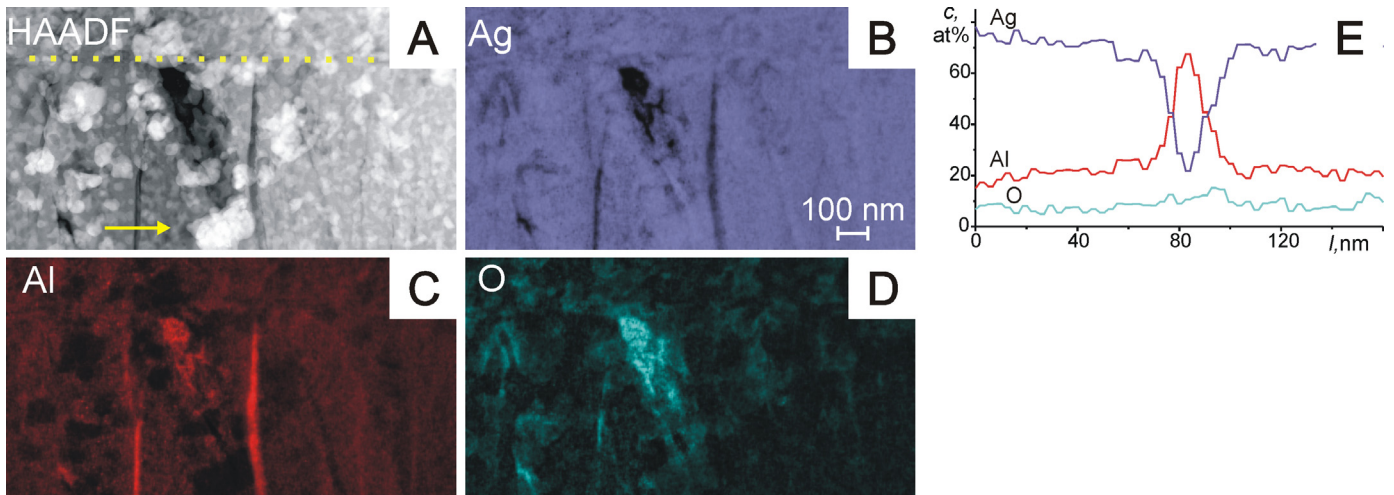

Fig. 3. HAADF image and EDX chemical element maps of the Ag–Al film. Line composition profile corresponds to the area highlighted with the arrow. Interface between tribofilm and as-deposited layer is marked with dot line

Fig. 5b). These planes are almost parallel to the surface of the lamellae, which means that the as-deposited film has (001) planes aligned parallel to the film surface. In order to identify the composition of nanosized precipitates, EDX spectrum from a particle located at the edge of the lamella has been recorded (Fig. 5e). It shows the presence of the Ag peaks only (minor peaks of Cu originate from TEM support grid), i.e. the precipitate phase is pure silver.

Therefore, combining results from STEM images, EDX maps and SAED patterns we may conclude that as-deposited Ag−Al film with Al content ca 25 at.% consists of hcp columnar grains with (001) planes aligned parallel to the film surface, accompanied by a pure Ag nanoparticle precipitates uniformly distributed over the whole thickness, and pores areas enriched with an aluminum oxide phase.

Development of morphology during growth of Ag−Al film could be described by the use of a structure-zone model [8-10].

In this model, the substrate temperature and the impurities are two main parameters, which directly control the morphological structure of the deposited film.

In the initial stage of the deposition process, nucleation of Ag−Al hcp islands on the surface of the Ti layer occurs via the Volmer-Weber mechanism, followed by their growth. Volume diffusion is almost "frozen" at room temperature of the substrate used in our experiments, therefore the coalescence of the growing grains is constrained. As a result, a growth competition between the neighboring crystals of different orientations is developed, leading to different growth rates of the crystal faces due to the surface energy anisotropy [8]. The surface energy anisotropy is related to the different number of broken bonds on the different crystal faces. The (001) surface of the hcp structure has the highest number of nearest-neighbors resulting in the lowest surface energy of this face. This is supported by the calculations of the surface energy of various surfaces for 13 hcp metals by using
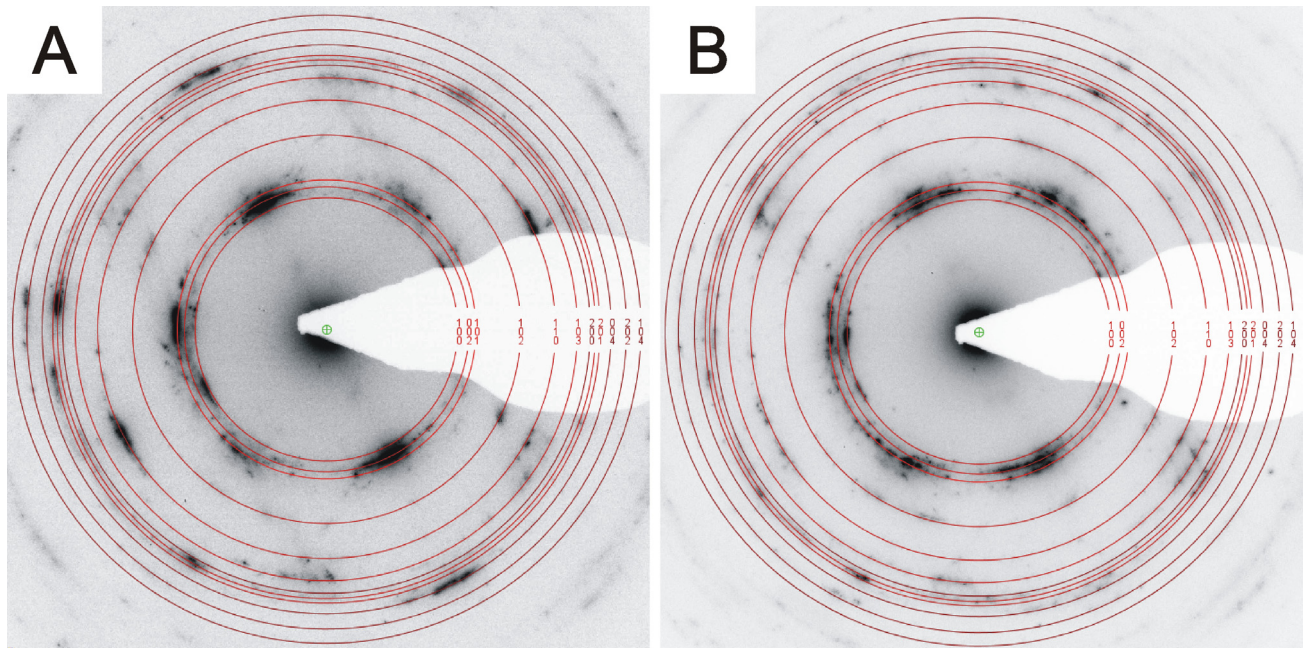
Fig. 4. Typical diffraction patterns (SAED) from the selected areas of the Ag–Al lamellae: a) as-deposited film and b) tribofilm area. Superimposed calculated rings correspond to the AgAl hcp phase
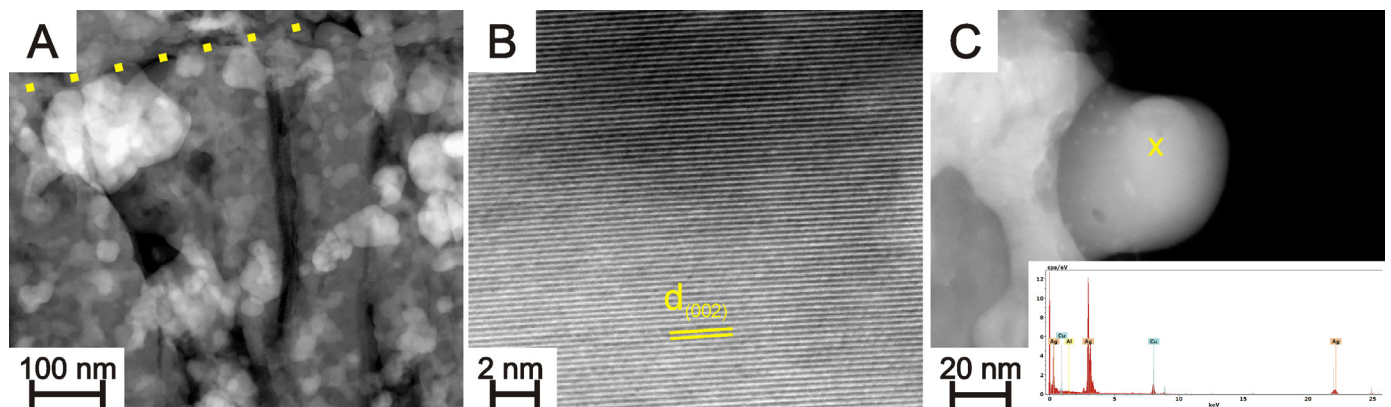

Fig. 5. HAADF-STEM images of the as-deposited Ag–Al film. Interface between tribofilm and as-deposited layer is highlighted with dot line. Inset in c) shows the EDX spectrum from the point marked with x

the modified embedded atom method [11]. Therefore, from the minimization of the surface energy, the (001) texture is favored during the hcp grain growth forming a columnar grain structure of the film, observed in Figures 2 and 5a.

On the other hand, the impurities from the residual atmosphere affect the development of the film morphology when the incident impurity to metal flux ratio J_i/J_m exceeds the value of 10^{-4} [10]. At a vacuum pressure of $\approx 10^{-8}$ Torr, one monolayer of residual gas molecules is formed within ≈ 100 s. Therefore, with the deposition speed of about one monolayer per second for Ag−Al alloy film, the J_i/J_m ratio has the value of $\sim 10^{-2}$. As a result, gas impurities have an influence on the structure formation during Ag−Al film growth. Impurities that are not soluble in the lattice are segregated into the grain boundaries and onto the growing film surface. At a critical impurity concentration, a passivation layer forms, upon which secondary nucleation occurs [9]. This process distorts the columnar shape of the grains

resulting in the film microstructure corresponding to zone T in the structure-zone model [8].

It should be noted, that the co-deposition is a highly non-equilibrium process generating plenty of defects and stresses in the growing film. Metastable oversaturated solid solutions are easily formed in case of deposition of binary films. E.g., the terminal solid-state solubility of sulfur in cadmium approaches the value of 18 at.% for S−Cd films deposited on a glass substrate at room temperature [12]. However, S and Cd are completely insoluble in the solid state according to the equilibrium phase diagram [13]. In the Ag−Al alloy film used in the study, the Ag content of 75 at.% exceeds the equilibrium composition of the hcp phase at room temperature (60-65 at.% Ag) [13], therefore an oversaturated solid solution is formed during the deposition process. This solid solution is not thermodynamically stable and a driving force exists to form a two-phase film with the hcp Ag–Al alloy and a more Ag-rich phase. Although, the phase diagram

suggests that other Ag-rich alloys exist such as Ag_3Al, these phases have a very complex structure and are therefore unlikely to form at the low deposition temperature used in our study. Hence, the kinetically most favorable phase composition is a mixture of hcp Ag–Al and fcc Ag in agreement with the TEM results.

In addition, the growing surface of the film generates a large number of non-equilibrium vacancies. These vacancies have no time to diffuse out of the condensation front and remain incorporated in the volume of the film. Thus, the concentration of non-equilibrium vacancies in a freshly deposited film can reach the value of 1% [14]. Diffusion of these vacancies and relaxation of internal stresses result in the formation of bubbles or pores within the solid of the film. They usually take on a spherical or cylindrical shape and are distributed uniformly throughout the film.

During the tribological tests, the columnar grain structure of the as-deposited film is destroyed and a tribofilm layer is formed on the film surface (Fig. 2). Thickness of this layer is not constant, its value gradually decreases from ca. 500 nm to 100 nm with the approaching to the center of the wear track. HAADF STEM studies of the tribofilm layer show that it consists of flattened grains, ranging in size between 5 to 100 nm (Fig. 6a). However, no significant change neither in distribution of chemical elements nor in phase composition has been detected. Diffraction patterns show the same Ag−Al hcp phase with somewhat weaker than in the as-deposited area texture (Fig. 4b). HRSTEM images of the grains in the body of the tribofilm (Fig. 6b) as well as on the wear surface (Fig. 6c) show that the observed texture is associated with a large portion of (001) planes aligned parallel to the film surface. Plenty of structural defects and lattice distortions are found in the tribofilm, however hcp phase has been identified in the majority of grains and boundaries. Thus, the shape and orientation of the grains in the tribofilm are conducive to the conclusion that the destruction of the hcp columns occurs on the easily sheared (001) planes of the hcp structure. These observations provide an insight into the phenomenon of significant reduction of the friction coefficient in hcp alloys and support the mechanism based on easy-shearing basal slip planes of hexagonal structure.

It should be noted that increased temperature and contact with ambient atmosphere promote formation of oxides in the wear track of Ag−Al alloy. These oxides may act as a lubricant,

significantly reducing the friction coefficients in the investigated frictional contact Ag/Ag-Al. E.g., the friction coefficient of aluminum oxide has the value of 0.2-0.25 [15], which is comparable with the measured friction coefficient of hcp Ag−Al phase (0.17) and it is possible that this can contribute to the low friction [3]. Therefore, particular attention has been paid to the study of oxygen distribution in the tribofilm zone. However, no oxide layer was detected on the surface of the film, the Ag−Al alloy directly contacts with the electron-beam deposited Pt protective layer (e-Pt) (Figs 2 and 6c). Nevertheless, an increased content of oxygen was found at grain boundaries and in nanosized voids between the grains of the tribofilm. Figure 7 shows the Ag, Al and O maps of the area I highlighted in Fig. 6a. One can see that in contrast to the distribution of oxygen atoms, the Al and Ag ones are uniformly distributed within grains. On the other hand, the boundaries are barely visible in the Al map, which means that Al atoms fill the voids between grains and may form an oxide phase. However, the high-resolution image of area II in Fig. 7a, which contains both Al and O atoms, shows no crystalline phase other than AgAl hcp one (Fig. 7d). It is also important to note that no correlation between oxygen atoms positions in the tribofilm and sliding direction has been found, i.e. there are no preferred directions of accumulation of Al and O atoms at grain boundaries. These observations do not allow us to exclude formation of amorphous lubricating oxides on the grain boundaries of Ag−Al tribofilm, however, they make it possible to claim that these oxides (if formed) have no dominant contribution to the reduced friction in Ag−Al hcp alloys.

4. Conclusions

It has been found that as-deposited Ag−Al alloy film (25 at.% Al) is composed of two polycrystalline phases, namely dominant hcp AgAl phase and a small amount of fcc Ag precipitates evenly distributed throughout the film thickness. A highly-textured AgAl hcp solid solution phase with (001) planes almost parallel to the film surface has a columnar grain microstructure corresponding to zone T in the structure-zone model.

Tribofilm with the thickness of a few hundred nanometers is formed in the wear track. AgAl hcp flattened grains with (001)
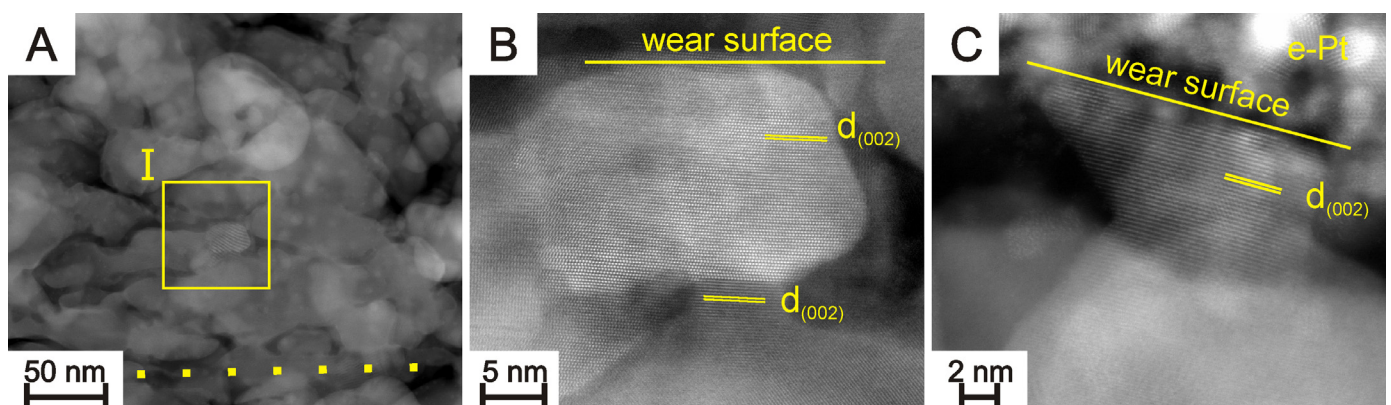

Fig. 6. HAADF-STEM images of different areas of the tribofilm. Direction of the wear surface is shown by solid line
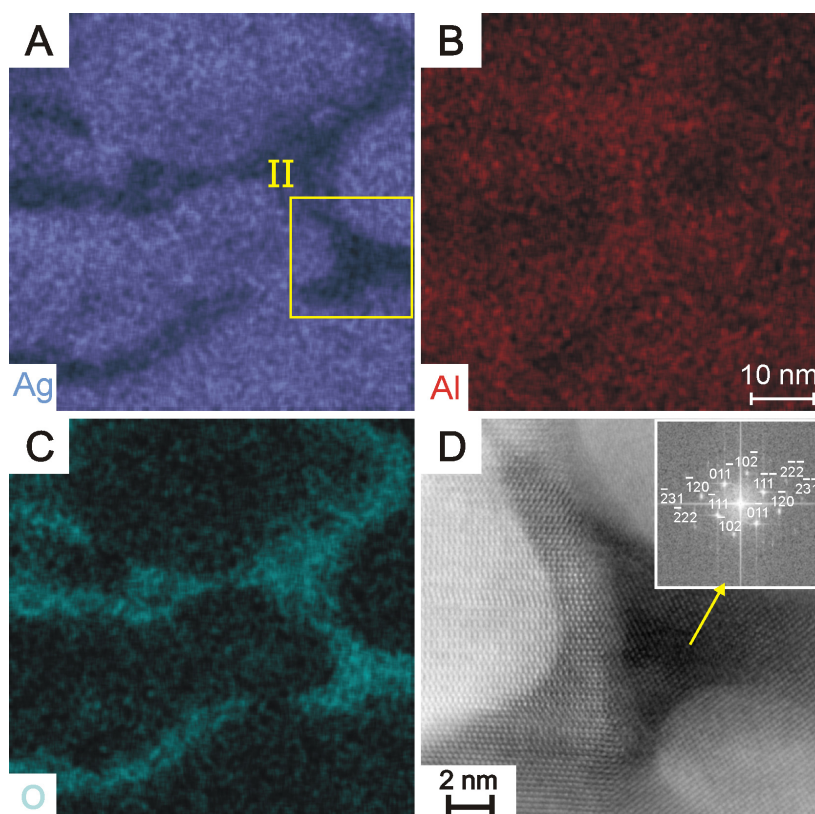
Fig. 7. EDX chemical element maps (a-c) of the Ag–Al tribofilm area shown in Fig. 6a. HAADF-STEM image (d) shows the highlighted area II in (a). The FFT shown in the inset corresponds to the [211] AgAl hcp phase

planes aligned parallel to the wear surface dominates in the microstructure of the tribofilm. Alignment of easy-shearing planes of a hexagonal structure is considered as a major mechanism of reduced friction in Ag−Al system.

REFERENCES

[1] F. Mao, U. Wiklund, A.M. Andersson, U. Jansson, J. Mater. Sci. **50**, 6518 (2015).

[2] F. Mao, M. Taher, O. Kryshtal, A. Kruk, A. Czyrska-Filemonowicz, M. Ottosson, A.M. Andersson, U. Wiklund, U. Jansson, ACS Applied Materials & Interfaces **8**, 30635 (2016).

[3] F. Mao, Doctoral thesis, Synthesis, Characterization, and Evaluation of Ag-based Electrical Contact Materials, Uppsala University, Sweden (2017). http://uu.diva-portal.org/smash/record.jsf?pid=diva2%3A1089132&dswid=-4657 accessed: 08 May 2018.

[4] M. Taher, F. Mao, P. Berastegui, A.M. Andersson, U. Jansson, Tribology International **119**, 680 (2018).

[5] D.H. Buckley, R.L. Johnson, Wear **11**, 405 (1968).

[6] E. Rabinowicz, Wear **159**, 89 (1992).

[7] P.A. Stadelmann. JEMS Java Electron Microscopy Software. http://www.jems-saas.ch accessed: 08 May 2018.

[8] P.B. Barna, M. Adamik, Growth mechanisms of polycrystalline thin films, in: F. C. Matacotta and G. Ottaviani (Eds.), Science and Technology of Thin Films, World Scientific, Singapore (1995).

[9] N. Kaiser, Appl. Opt. **41**, 3053-60 (2002).

[10] I. Petrov, P.B. Barna, L. Hultman, J.E. Greene, J. Vac. Sci. Technol. A **21**, S117 (2003)

[11] J.M. Zhang, D.D. Wang, K.W. Xu, Appl. Surf. Sci. **253**, 2018 (2006)

[12] N.T. Gladkikh, S.V. Dukarov, A.P. Kryshtal', V.I. Larin., V.N. Sukhov, S.I. Bogatyrenko, Poverkhnostnye yavleniya i fazovye prevrashcheniya v kondensirovannykh plenkakh (Surface Phenomena and Phase Transformations in Condensed Films), Kharkov: Izd-vo KhNU (2004), http://dspace.univer.kharkov.ua/handle/123456789/11158 accessed 08 May 2018.

[13] H. Okamoto, Phase Diagrams for Binary Alloys. Desk Handbook, ASM International, USA (2000).

[14] G.P. Zhigal'skii, B.K. Jones, The Physical Properties of Thin Metal Films, Taylor & Francis, London & New York (2003).

[15] Smithells Metals Reference Book, E.A. Brandes and G.B. Brook (Eds.), 7th edn., Butterworth-Heinemann (1992).